Direct oxidation of methane at low temperature using Pt/C, Pd/C, Pt/C-ATO and Pd/C-ATO electrocatalysts prepared by sodium borohydride reduction process

J. Nandenha, E. H. Fontes, R. M. Piasentin, F. C. Fonseca, A. O. Neto*
(*Instituto de Pesquisas Energéticas e Nucleares, IPEN/CNEN-SP, Av. Prof. Lineu Prestes, 2242 Cidade Universitária, CEP* 05508-000, *São Paulo, SP, Brazil*)

Abstract: The main objective of this paper was to characterize the voltammetric profiles of the Pt/C, Pt/C-ATO, Pd/C and Pd/C-ATO electrocatalysts and study their catalytic activities for methane oxidation in an acidic electrolyte at 25 ℃ and in a direct methane proton exchange membrane fuel cell at 80 ℃. The electrocatalysts prepared also were characterized by X-ray diffraction (XRD) and transmission electron microscopy (TEM). The diffractograms of the Pt/C and Pt/C-ATO electrocatalysts show four peaks associated with Pt face-centered cubic (fcc) structure, and the diffractograms of Pd/C and Pd/C-ATO show four peaks associated with Pd face-centered cubic (fcc) structure. For Pt/C-ATO and Pd/C-ATO, characteristic peaks of cassiterite (SnO_2) phase are observed, which are associated with Sb-doped SnO_2(ATO) used as supports for electrocatalysts. Cyclic voltammograms (CV) of all electrocatalysts after adsorption of methane show that there is a current increase during the anodic scan. However, this effect is more pronounced for Pt/C-ATO and Pd/C-ATO. This process is related to the oxidation of the adsorbed species through the bifunctional mechanism, where ATO provides oxygenated species for the oxidation of CO or HCO intermediates adsorbed in Pt or Pd sites. From in situ ATR-FTIR (Attenuated Total Reflectance-Fourier Transform Infrared) experiments for all electrocatalysts prepared the formation of HCO or CO intermediates are observed, which indicates the production of carbon dioxide. Polarization curves at 80 ℃ in a direct methane fuel cell (DMEFC) show that Pd/C and Pt/C electroacatalysts have superior performance to Pd/C-ATO and Pt/C-ATO in methane oxidation.

Key words: sodium borohydride reduction process; Pt/C-ATO and Pd/C-ATO electrocatalysts; methane oxidation; acidic electrolytes; polarization curves

CLC number: O643.3 **Document code**: A

Methane is the main constituent of natural gas widely used as fuel in the industry and in private households, where it has been exerted a profound economic and sociologic influence on the world at large because of its enormous reserves[1,2]. The methane (CH_4) can also be generated from renewable sources like biomass, solid organic waste, landfill gas. Consequently, methane is among the simplest and readily available organic compounds that could be used in a fuel cell[3].

In the fuel cell, the methane could be used after steam reforming or directly in solid oxide fuel cell[4]. The high operating temperature of a solid oxide fuel cell (SOFC) leads to problems, like carbon deposition, and requires high startup time, consequently the use of methane directly in a proton exchange membrane fuel cell (PEMFC) would avoid these problems. So, it′s necessary to select electrocatalysts to be used in a direct methane fuel cell (DMEFC).

The activation of C−H and C−C bonds in small hydrocarbons by various transition metal oxide ions has been investigated experimentally and theoretically by several authors[5−10]. Berthelot et al[11] showed that electro-oxidation of methane could be carried out using Pt or Pt-Ru as electrocatalysts, where they reported that carbon dioxide was produced for Pt and methanol resulted when using Pt-Ru.

Platinum (Pt) is widely used in electrochemical reactions because of its higher electrocatalytic activity than other metals. However, the limitation of use of the Pt electrocatalysts comes from the high cost and limited resources of Pt. Consequently, the use of palladium (Pd) and Pd group metals are frequently employed as anodic electrodes for the electrochemical oxidation of methane, because Pd is at least fifty times more available than Pt in the earth[12,13]. Joglekar et al[14] showed the development of platinum organometallic complexes covalently anchored to ordered mesoporous carbon (OMC) for

Received: 2018-05-17; Revised: 2018-07-24.

* Corresponding author. Tel: +55-11-3133-9284, Fax: +55-11-3133-9285, E-mail: aolivei@ipen.br, neto.almir@bol.com.br.

The project was supported by the FAPESP (2014/09087-4, 2014/50279-4).

本文的英文电子版由 Elsevier 出版社在 ScienceDirect 上出版(http://www.sciencedirect.com/science/journal/18725813).

electrochemical oxidation of methane in a proton exchange membrane fuel cell at 80 ℃, where was obtained a power density of 403 μW/mg Pt, which was five times higher than the power density observed from a modern commercial catalyst and two orders of magnitude higher than that from a Pt black catalyst.

In another study, Neto et al[15] prepared a Pt supported on $Sb_2O_5 \cdot SnO_2$ (ATO) with various amounts of Pt loaded on ATO and tested for methanol and ethanol electro-oxidation using electrochemical techniques. The activities of Pt/ATO for methanol and ethanol electro-oxidation were higher than those of Pt/C, where the enhancement of activity was attributed to better dispersion of Pt nanoparticles on the ATO support, as well as to the effects of SnO_2 adjacent to Pt.

Li et al[16] synthesized Palladium nanoparticles (PdNPs) using *n*-alkylamines (C_n-NH_2) as stabilizing ligands. These authors showed that the PdNPs were more activity and stable response to CH_4 when compared to the bare Pd electrodes.

Agarwal et al[17] showed that PdAu nanoparticles supported on titanium oxide had high selectivity (92%) for oxidized methane to methanol in aqueous solution at mild temperatures.

This work aimed to prepare Pt/C, Pt/C-ATO, Pd/C and Pd/C-ATO electrocatalysts by sodium borohydride reduction process for methane oxidation in acidic electrolytes. This work includes not only electrochemical experiments but also single-cell experiments.

1 Experimental

Pt/C, Pt/C-ATO, Pd/C and Pd/C-ATO electrocatalysts were prepared using $H_2PtCl_6 \cdot 6H_2O$ (chloroplatinic acid - Aldrich) and $Pd(NO_3)_2 \cdot 2H_2O$ (Fluka) as metal sources and sodium borohydride ($NaBH_4$, Aldrich) as reducing agent. For Pt/C-ATO and Pd/C-ATO, a physical mixture of 85% Vulcan Carbon XC72 and 15% ATO ($Sb_2O_5 \cdot SnO_2$- Aldrich, nanopowder, < 50 nm, composition (by weight): 7%–11% Sb_2O_5 and 89%–93% SnO_2) was used as support, this proportion was chosen according to reference[15]. The 100% Vulcan XC72 or 85% Vulcan XC72-15% ATO support were dispersed into a solution of water/2-propanol (50/50, volume ratio), containing metal ions of Pd or Pt. The mixture resulting was submitted to an ultrasonic bath and a $NaBH_4$ solution in 0.01 mol/L NaOH was added in one step under stirring at room temperature, and the resulting solution was then maintained under stirring for an additional 30 min[18]. Finally, the material was filtered, washed with ultrapure water and dried at 70 ℃ for 2 h.

X-ray diffraction (XRD) analysis of Pt/C, Pt/C-ATO, Pd/C and Pd/C-ATO electrocatalysts were obtained in a Rigaku Diffractometer model Miniflex II using Cu $K\alpha$ radiation source (λ = 0.15406 nm). All diffractograms were recorded in the range of 2θ = 20° to 90° with a step size of 0.05° and a scan time of 2 s per step. The morphology, distribution, and size of Pt/C, Pt/C-ATO, Pd/C and Pd/C-ATO nanoparticles were determined in a JEOL electron microscope model JEM-2100 operated at 200 kV by measuring 205 nanoparticles from 10 micrographs.

The cyclic voltammetry of Pt/C, Pt/C-ATO, Pd/C and Pd/C-ATO electrocatalysts were carried out with an AutoLab PGSTAT30 Potentiostat, at 25 ℃ in a 0.5 mol/L H_2SO_4 solution using a three-electrodes conventional cell. The reference electrode was a reversible hydrogen electrode (RHE), Pt wire was utilized as a counter electrode and thin porous coating technique as work electrode as previously reported[18]. The cyclic voltammetry experiments were done at a scan rate of 10 mV/s for the potential range of 0.05 to 1.2 V with the presence or absence of methane. The adsorption of methane was realized at 0.05 V with bubbling for 30 min in 0.5 mol/L H_2SO_4.

The spectroelectrochemical ATR-FTIR in situ measurements were performed on a Nicolet 6700 FT-IR spectrometer equipped with an MCT detector cooled with liquid N_2, ATR accessory (MIRacle with a Diamond/ZnSe Crystal Plate Pike®), and an electrochemical cell. The working electrodes were ultrathin porous coating technique in the presence of methane and 0.5 mol/L H_2SO_4. The absorbance spectra were collected at the ratio $R : R_0$, where R represents a spectrum at a given potential and R_0 is the spectrum obtained at 0.05 V, where positive and negative directional bands represent gain and loss of species at the sampling potential, respectively. The spectra were computed from 128 interferograms averaged from 3250 to 850 cm^{-1} with the spectral resolution set to 8 cm^{-1}, and the sample spectra were collected after applying potential successive steps from 0.1 V, from 0.05 to 1.2 V.

The direct methane fuel cell performances were determined in a single cell with an area of 5 cm^2. The temperatures were set to 80 ℃ for the fuel cell and 85 ℃ for the methane humidifier and 85 ℃ for the oxygen humidifier. The fuel was 500 mL of 99% methane gas at approximately 200 mL/min, the oxygen flow was regulated at 200 mL/min and pressure atmospheric. Polarization curves were obtained using an AutoLab PGSTAT302N Potentiostat connected in the fuel cell, and a panel of cell

experiments was used-Electrocell® Group. Membrane Electrode Assemblies (MEAs) were prepared by hot pressing of a pretreated Nafion® 117 membranes placed between Pt/C, Pt/C-ATO, Pd/C and Pd/C-ATO electrocatalysts. The anode prepared in this work was made of 1 $mg_{(Pt)}/cm^2$ electrocatalyst loading. The cathodic electrocatalyst was made of 20% Pt/C BASF and 1 $mg_{(Pt)}/cm^2$ electrocatalyst loading. After this, they were pressed at 125 ℃ for 2 min under pressure of 225 kgf/cm^2.

2 Results and discussion

The X-ray diffractograms of the Pt/C, Pt/C-ATO, Pd/C and Pd/C-ATO electrocatalysts are shown in Figure 1. For all electrocatalysts prepared are observed a broad peak at about $2\theta \approx 25°$ that are associated with the Vulcan Carbon XC72 support material. For Pt/C and Pt/C-ATO electrocatalysts are observed four peaks at approximately $2\theta \approx 40°$, 47°, 67° and 82°, which are associated with the (111), (200), (220) and (311) planes, respectively, characteristic of Pt face-centered cubic (fcc) structure JCPDS Card #40-802[19]. For Pd/C and Pd/C-ATO electrocatalysts are observed at $2\theta \approx 40°$, 47°, 67° and 82°, which are associated with crystal planes (111), (200), (220) and (311) corresponding to the face-centered cubic structure of palladium JCPDS 46-1043[20]. For Pt/C-ATO and Pd/C-ATO are also observed peaks at about $2\theta \approx 27°$, 34°, 38°, 52°, 55°, 62°, 65° and 66°, which are characteristic of cassiterite (SnO_2) phase[15].

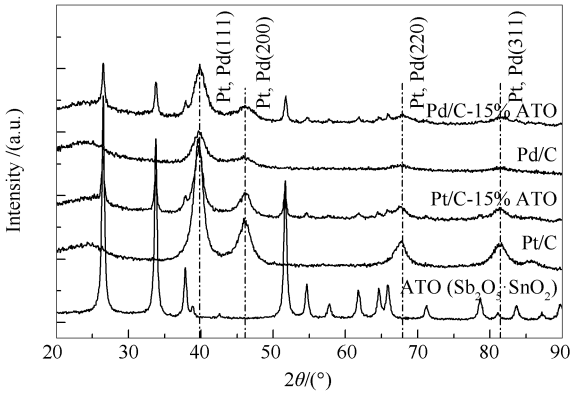

Figure 1　X-ray diffractograms of Pt/C, Pt/C-ATO, Pd/C and Pd/C-ATO electorcatalysts

The micrographs and histograms of the nanoparticle size distribution, obtained by TEM for Pt/C, Pt/C-ATO, Pd/C and Pd/C-ATO electrocatalysts are illustrated in Figures 2 and 3. The mean diameter of the nanoparticles for Pt/C, Pt/C-ATO, Pd/C and Pd/C-ATO are in the range of 6.4 −8.1 nm. All electrocatalysts prepared show a good distribution of the nanoparticles on the carbon support and the morphologies are not significantly changed. The nanoparticles sizes of the Pt/C and Pd/C are smaller than those of Pt/C-ATO and Pd/C-ATO, respectively in accordance with the results of Neto et al works[15,21].

Cyclic voltammograms of Pt/C, Pt/C-ATO, Pd/C and Pd/C-ATO electrocatalysts before and after adsorption of methane at 0.05 V while bubbling methane for 30 min in 0.5 mol/L H_2SO_4 are shown in Figure 4. For Pt/C and Pt/C-ATO electrocatalysts it is observed that the hydrogen adsorption-desorption regions increase partially in comparison with cyclic voltammograms before adsorption of methane. This indicates the presence of oxygen species covering the electrode surface. It is also observed an increase in current during the anodic scan which presumably corresponds to the oxidation of the adsorbed species. This effect is more pronounced for Pt/C-ATO which indicates that the presence of the ATO favors the oxidation of methane to other products of higher commercial values. These results are partially following the work of Hahn et al[3].

For Pd/C and Pd/C-ATO it is observed a formation of PdOH (Pd_2O) at 0.60 V and it is further oxidized to PdO at 0.90 V. The oxidation peak increases after the adsorption of methane, and the reduction peak current at 0.70 V doesn't vary, which indicates that the oxidation process is irreversible. The oxidation peak increment is more pronounced for Pd/C-ATO indicating that the presence of ATO favors the oxidation of methane toward intermediates species, such as CO or −CHO, and toward products, such as CO_2. This result also indicates higher electron transfer rate for methane oxidation at the Pd/C-ATO electrode than that at the Pd/C. For Pd/C and Pd/C-ATO it is also observed that the hydrogen adsorption-desorption increases dramatically in comparison with Pt/C and Pt/C-ATO cyclic voltammograms after adsorption of methane. This indicates the presence of many oxygen species covering the electrode surface.

Finally, for Pd/C and Pd/C-ATO it is also observed a partially suppressed hydrogen adsorption peak, which is an indication of the presence of another species on the electrode surface. Pd/C and Pd/C-ATO results are partly following the work of Zhang et al[2].

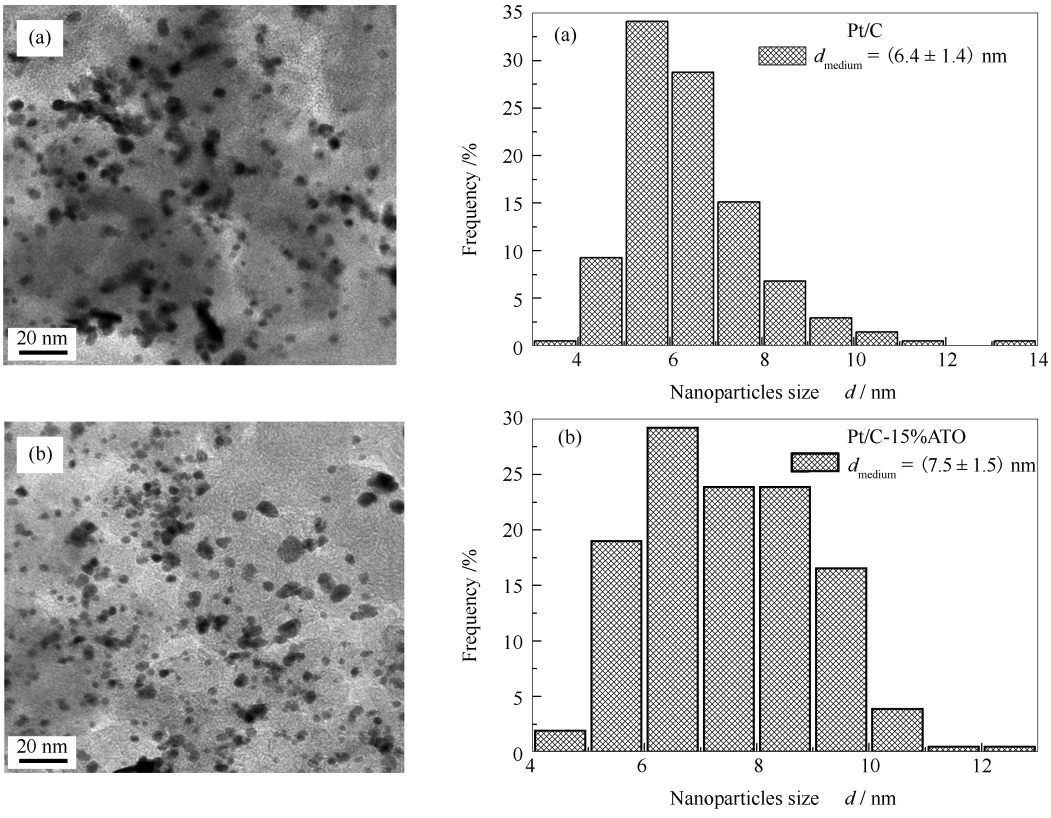

Figure 2 TEM images and histograms of the nanoparticles size distribution to Pt/C (a) and (b) Pt/C-ATO electrocatalysts

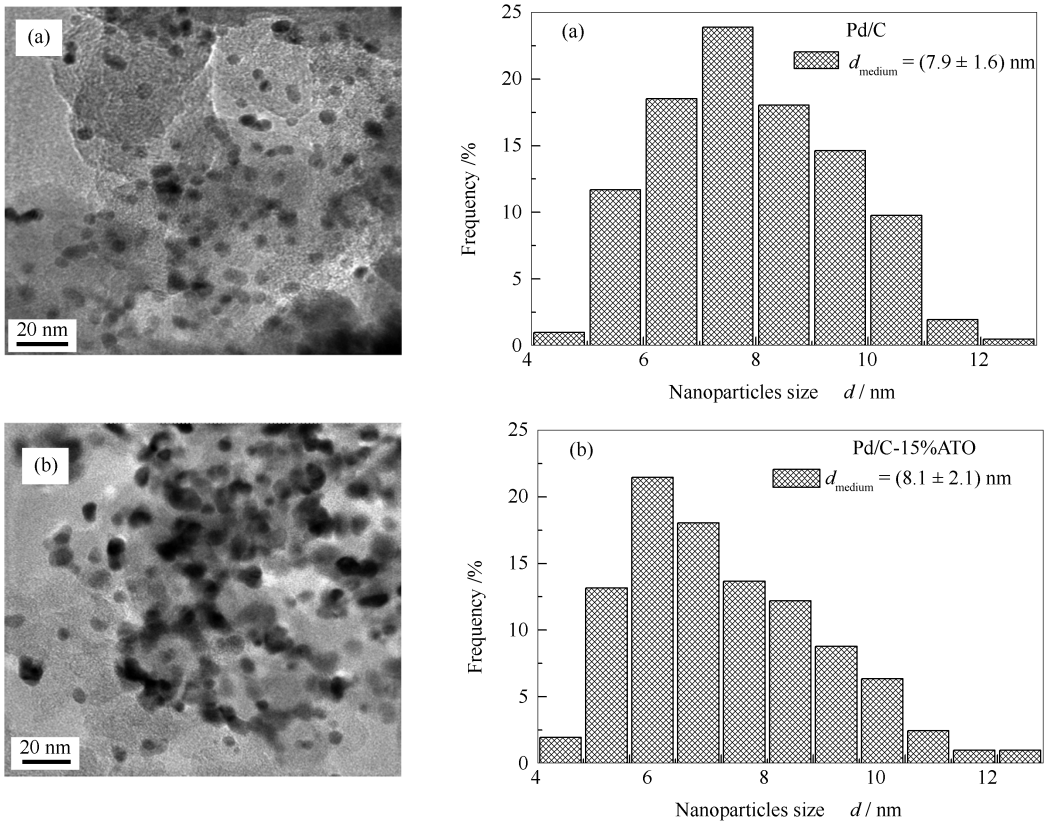

Figure 3 TEM images and histograms of the nanoparticles size distribution to Pd/C (a) and (b) Pd/C-ATO electrocatalysts

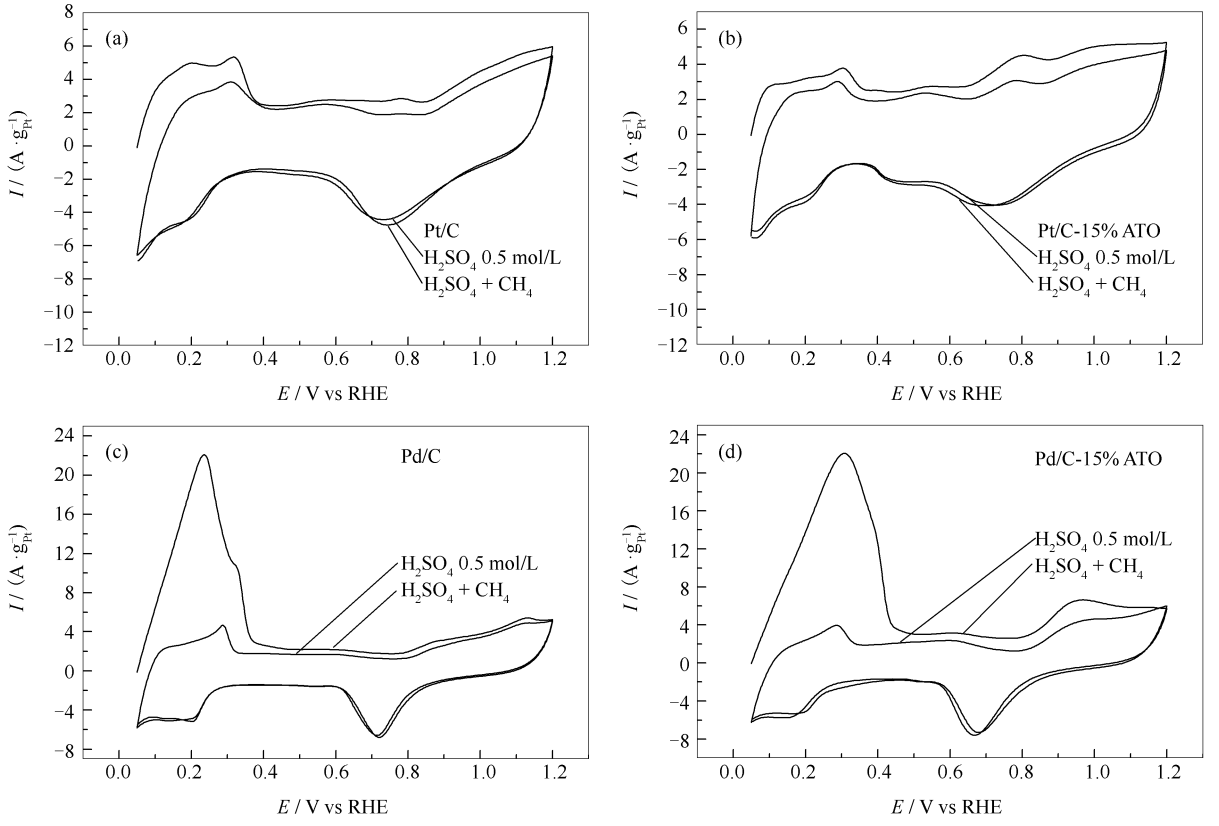

Figure 4　Comparison of the current-potential curves for (a) Pt/C, (b) Pt/C-ATO, (c) Pd/C and (d) Pd/C-ATO electrodes in the absence of methane and methane (CH_4) passing through the 0.5 mol/L H_2SO_4 electrolyte for 30 min

Figures 5 and 6 display in situ ATR-FTIR spectra in the range of 3250 to 850 cm^{-1} of electrochemical oxidation of methane on Pt/C, Pt/C-15% ATO, Pd/C and Pd/C-15% ATO electrocatalysts at potentials range from 0.05 to 1.2 V with step of 0.1 V. It is possible to observe the presence of methane for all electrocatalysts studied. Its appearance is due to the degenerate deformation f_2 (deg deform. f_2) band approximately in 1306 cm^{-1}, degenerate deformation e (deg deform. e) band in about 1533 cm^{-1} and degenerate stretching f_2 (deg stret. f_2) band in approximately 3019 cm^{-1}[22]. All materials, except Pd/C, exhibited peaks in 1045, 2177 and 2600 cm^{-1}. They are respectively associated with CO stretching in a CO matrix (CO str CO matrix)[23,24], CO stretching in a gas environment (CO str gas)[23,24] and CH stretching in a gas environment (CH str gas)[25] of the intermediate species (–CHO and CO). The carbon dioxide band is removed because the interference of CH_4 gas in the in situ experiment is too high. It should be noticed that in Figures 5(a.1, b.2) and 6(d.2) all the bands have similar variations, indicating that –CHO or CO are produced in near potentials. Also, this can be a good indicator of CO_2 production[23]. For high potentials, Pt/C and Pt/C-15% ATO electrocatalysts have shown a good agreement between CV experiments and FT-IR measurements. CO str CO matrix and CO str gas increased linearly, while the current density also has grown. Pd/C also doesn't show any intermediate products for the potentials studied, which agrees with CV results, because the CV results using H_2SO_4 solution is very similar to CV using H_2SO_4 plus CH_4 solution. Besides all that, we can notice that ATO plays a decisive role in the electrocatalytic activity. Pd/C-15% ATO produces intermediate products, while Pd/C doesn't.

Hahn et al[3] showed for Pt that the final product observed was CO_2, and CO, –CHO (aldehyde) or –COOH (acid) species were identified as reaction intermediates. These authors concluded that the activation of methane at room temperature was nevertheless possible using noble metals as electrocatalysts. For Pd CO_2 was also observed as final product, however, the detection of –CHO or –COOH species did not yield definitive results[3]. These authors also suggested that the use of SEIRAS (Surface-Enhanced Infrared Absorption Spectroscopy) technique was more appropriate to investigate in-situ methane oxidation than that of a

conventional FT-IR spectroscopy.

Figure 7 shows the polarization and power density curves obtained in a single direct methane fuel cell using Pt/C, Pt/C-ATO, Pd/C and Pd/C-ATO as anode electrocatalysts. Pd/C electrocatalyst is more active than Pt/C, Pd/C-ATO and Pt/C-ATO prepared. This result is not in agreement with that obtained using CV experiments, in which Pt/C-ATO and Pd/C-ATO are more active for methane oxidation. The disagreement between electrochemical experiments and direct methane fuel cell results could be attributed to different experimental conditions of conventional CV and fuel cell, which are the diffusion of the fuel through the catalytic layer, the continuous and constant flow, and the temperature. Our results show that new studies with new membranes, new diffuser layers, and new electrocatalysts are necessary for the development of direct methane fuel cells (DMEFCs).

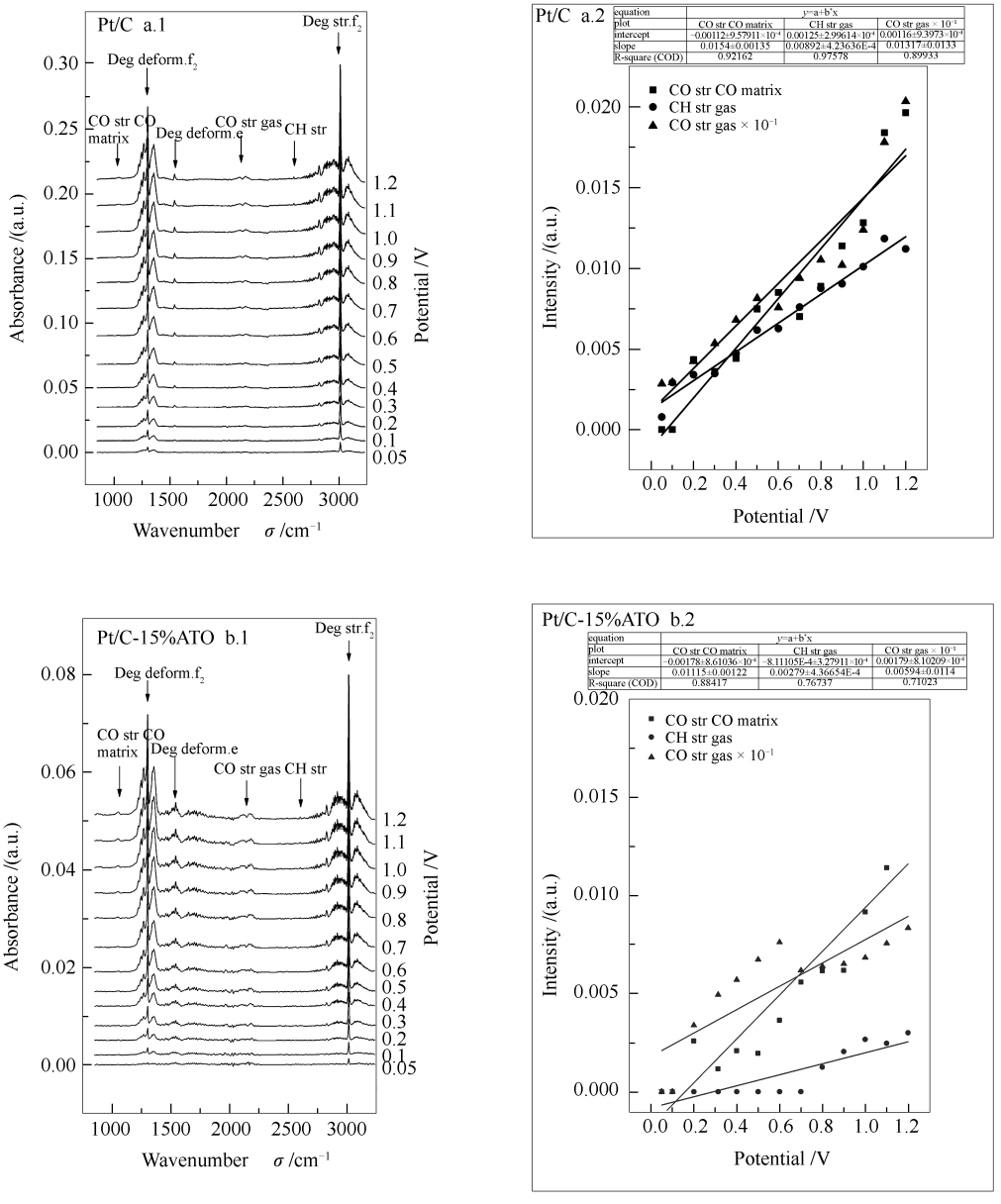

Figure 5 In situ ATR-FTIR spectra and integrated bands in the range of 3250 to 850 cm^{-1} of electrochemical oxidation of methane on Pt/C and Pt/C-ATO electrocatalysts at potentials range from 0.05 to 1.2 V with an interval of 0.1 V

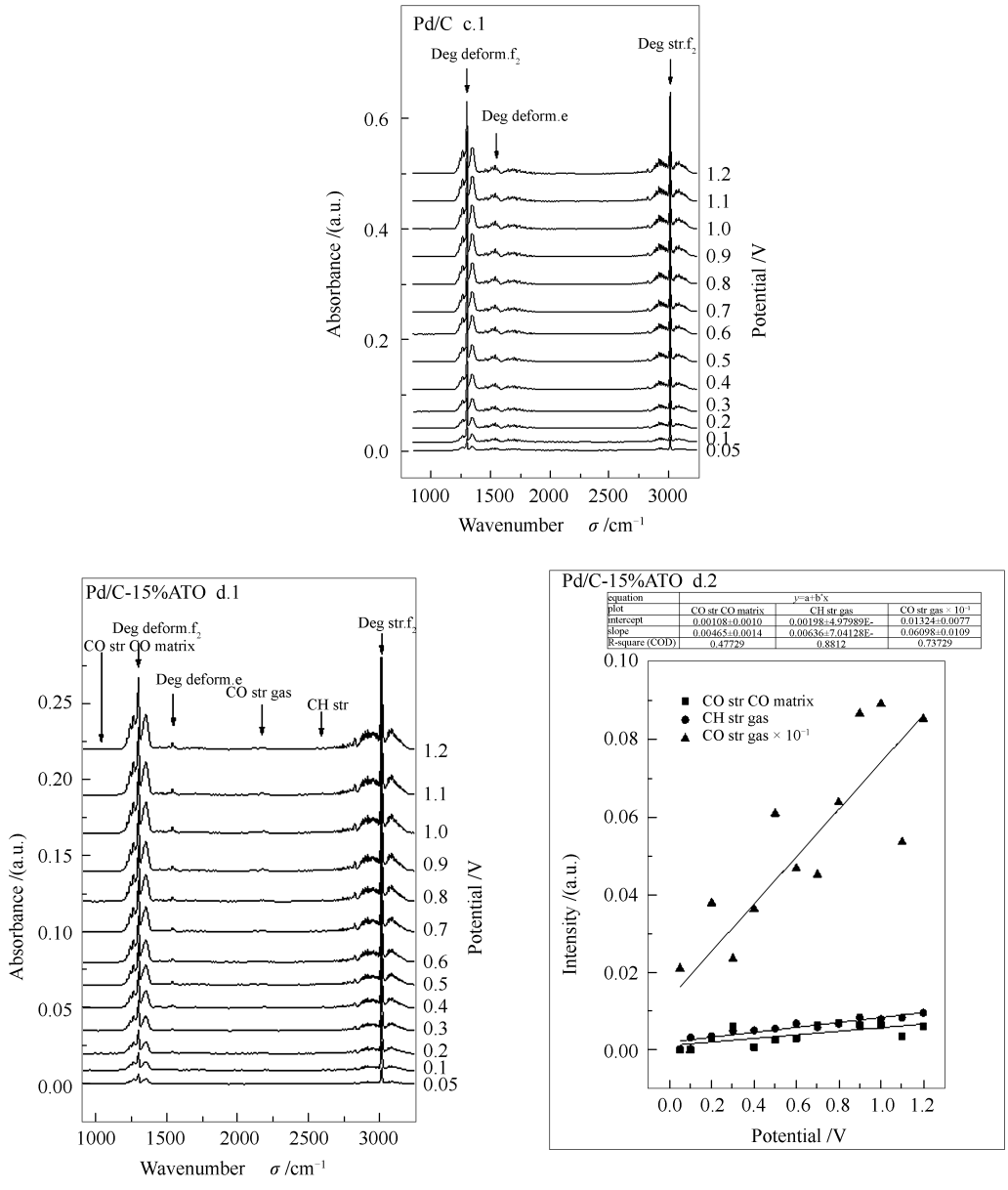

Figure 6　In situ ATR-FTIR spectra and integrated bands in the range of 3250 to 850 cm^{-1} of electrochemical oxidation of methane on Pd/C and Pd/C-ATO electrocatalysts at potentials range from 0.05 to 1.2 V with an interval of 0.1 V

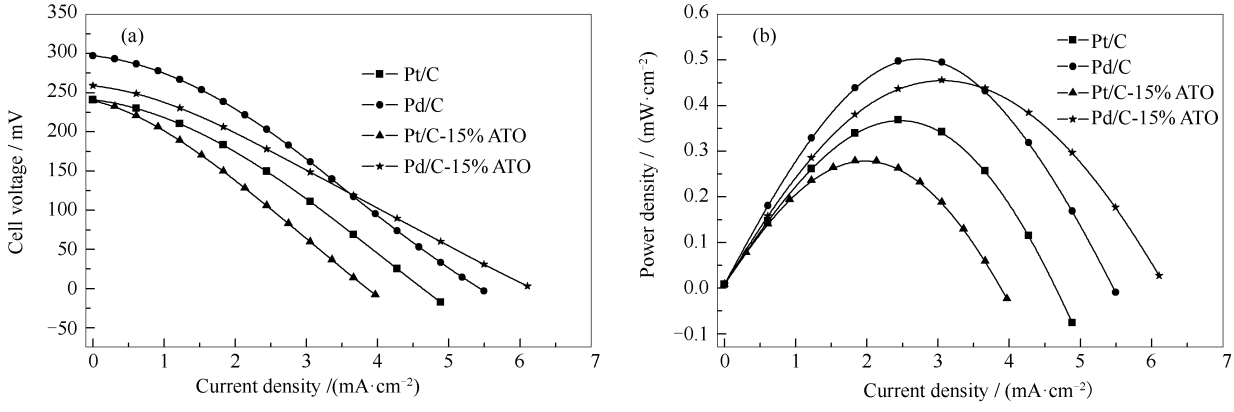

Figure 7　(a) Polarization and (b) power density curves of a 5 cm^2 direct methane fuel cell at 80 ℃ using 200 mL of methane

3 Conclusions

The sodium borohydride reduction method is an efficient process to produce Pt/C, Pt/C-ATO, Pd/C and Pd/C-ATO electrocatalysts for methane oxidation. Pt/C and Pt/C-ATO electrocatalysts show four peaks associated with Pt face-centered cubic (fcc) structure, and Pd/C and Pd/C-ATO electrocatalysts show four peaks associated with Pd face-centered cubic (fcc) structure. Pt/C-ATO and Pd/C-ATO are also observed peaks characteristic of cassiterite (SnO_2) phase, which are associated with Sb-doped SnO_2(ATO) support.

It is possible to observe the presence of intermediate species, like CO or –CHO, which indicates the presence of carbon dioxide species coming from methane oxidation.

The disagreement between electrochemical experiments and direct methane fuel cell results could be associated with different settings used in a conventional CV and fuel cell. Pd/C and Pt/C show superior performance for methane oxidation in direct methane fuel cell, while Pd/C-ATO and Pt/C-ATO indicated a decrease in kinetics reaction that is why Pd/C has a better open circuit voltage.

Acknowledgments

The authors thank the Laboratório de Microscopia do Centro de Ciências e Tecnologia de Materiais (CCTM) by TEM measurements.

References

[1] JACQUINATA P, MÜLLER B, WEHRLI B, HAUSER P C. Determination of methane and other small hydrocarbons with a platinum-Nafion electrode by stripping voltammetry[J]. Anal Chim Acta, 2001, **432**(1): 1–10.

[2] ZHANG Y, ZHANG L, SHUANG S, FENG F, QIAO J, GUO Y, CHOI Y, MARTIN M F, DONG C. Electro-oxidation of methane on roughened palladium electrode in acidic electrolytes at ambient temperatures[J]. Anal Lett, 2010, **43**(6): 1055–1065.

[3] HAHN F, MELENDRES C A. Anodic oxidation of methane at noble metal electrodes: An 'in situ' surface enhanced infrared spectroelectrochemical study[J]. Electrochim Acta, 2001, **46**(23): 3525–3534.

[4] TYAGIA S, GANESH A, AGHALAYAM P. Direct methane proton exchange membrane fuel cell[J]. ECS Trans, 2008, **6**(25): 371–378.

[5] HWANG D Y, MEBEL A M. Activation of methane by neutral transition metal oxides (ScO, NiO, and PdO): A Theoretical Study[J]. J Phys Chem A, 2002, **106**(50): 12072–12083.

[6] SCHRÖDER D, SCHWARZ H. FeO ⊕ activates methane[J]. Angew Chem, Int Ed Eng, 1990, **29**(12): 1433–1434.

[7] SCHRÖDER D, SCHWARZ H. C–H and C–C bond activation by bare transition-metal oxide cations in the gas phase[J]. Angew Chem, Int Ed Eng, 1995, **34**(18): 1973–1995.

[8] CLEMMER D E, CHEN Y M, KAHN F A, ARMENTROUT P B. State-specific reactions of Fe+(a6D,a4F) with D2O and reactions of FeO+ with D2[J]. J Phys Chem, 1994, **98**(26): 6522–6529.

[9] SIEGBAHN P E M. Comparison of the C–H activation of methane by $M(C_5H_5)(CO)$ for M = cobalt, rhodium, and iridium[J]. J Am Chem Soc, 1996, **118**(6): 1487–1496.

[10] WITTBORN A M C, COSTAS M, BLOMBERG M R A, SIEGBAHN P E M. The C–H activation reaction of methane for all transition metal atoms from the three transition rows[J]. J Chem Phys, 1997, **107**(11): 4318–4328.

[11] BERTHELOT S, GEHAIN E, HAHN F, LÉGER J M, SRINIVASAN S, LAMY C. Extended Abstracts, Electrochemical Society Meeting, Boston, 98–2, 1998, Abstract 1090.

[12] BENSEBAA F, FARAH A A, WANG D, BOCK C, DU X, KUNG J, PAGE Y L. Microwave synthesis of polymer-embedded Pt-Ru catalyst for direct methanol fuel cell[J]. J Phys Chem B, 2005, **109**(32): 15339–15344.

[13] SAVADOGO O, LEE K, OISHI K, MITSUSHIMA S, KAMIYA N, OTA K I. New palladium alloys catalyst for the oxygen reduction reaction in an acid medium[J]. Electrochem Commun, 2004, **6**(2): 105–109.

[14] JOGLEKAR M, NGUYEN V, PYLYPENKO S, NGO C, LI Q, O′REILLY M E, GRAY T S, HUBBARD W A, GUNNOE T B, HERRING A M, TREWYN B G. Organometallic complexes anchored to conductive carbon for electrocatalytic oxidation of methane at low temperature[J]. J Am Chem Soc, 2016, **138**(1): 116–125.

[15] NETO A O, BRANDALISE M, DIAS R R, AYOUB J M S, SILVA A C, PENTEADO J C, LINARDI M, SPINACÉ E V. The performance of Pt nanoparticles supported on $Sb_2O_5 \cdot SnO_2$, on carbon and on physical mixtures of $Sb_2O_5 \cdot SnO_2$ and carbon for ethanol electro-oxidation[J]. Int J Hydrogen Energy, 2010, **35**(17): 9177–9181.

[16] LI Z, GAO J, XING X, WU S, SHUANG S, DONG C, PAAU M C, CHOI M M F. Synthesis and characterization of *n*-alkylamine-stabilized palladium nanoparticles for electrochemical oxidation of methane[J]. J Phys Chem C, 2010, **114**(2): 723–733.

[17] AGARWAL N, FREAKLEY S J, MCVICKER R U, ALTHAHBAN S M, DIMITRATOS N, HE Q, MORGAN D J, JENKINS R L, WILLOCK D J, TAYLOR S H, KIELY= C J, HUTCHINGS G J. Aqueous Au-Pd colloids catalyze selective CH4 oxidation to CH_3OH with O_2 under mild conditions[J]. Science, 2017, **358**(6360): 223–227.

[18] DA SILVA S G, FONTES E H, ASSUMP O M H M T, LINARDI M, SPINACÉ E V, SILVA J C M, NETO A O. Fuel cell and electrochemical studies of the ethanol electro-oxidation in alkaline media using PtAuIr/C as anodes[J]. Ionics, 2017, **23**(9): 2367–2376.

[19] MAYA-CORNEJO J, CARRERA-CERRITOS R, SEBASTÍAN D, LEDESMA-GARCÍA J, ARRIAGA L G, ARICÒ A S, BAGLIO V.

PtCu catalyst for the electro-oxidation of ethanol in an alkaline direct alcohol fuel cell[J]. Int J Hydrogen Energy, 2017, **42**(46): 27919-27928.

[20] GUO J, CHEN R, ZHU F C, SUN S G, VILLULLAS H M. New understandings of ethanol oxidation reaction mechanism on Pd/C and Pd_2Ru/C catalysts in alkaline direct ethanol fuel cells[J]. Appl Catal B: Environ, 2018, **224**(5): 602-611.

[21] OTTONI C A, DE SOUZA R R, DA SILVA S G, SPINACÉ E V, DE SOUZA R F B, NETO A O. Performance of Pd electrocatalyst supported on a physical mixture indium tin oxide-carbon for glycerol electro-oxidation in alkaline media[J]. Electroanalysis, 2017, **29**(4): 960-964.

[22] SHIMANOUCHI T. National Bureau of Standards. 1972, 1-160.

[23] HAHN F, MELENDRES C A. Anodic oxidation of methane at noble metal electrodes: An 'in situ' surface enhanced infrared spectroelectrochemical study[J]. Electrochimica Acta, 2001, **46**(23): 3525-3534.

[24] MILLIGAN D E, JACOX M E. Matrix-isolation study of the infrared and ultraviolet spectra of the free radical HCO. The hydrocarbon flame bands. [J]. J Chem Phys, 1969, **51**(1): 277-288.

[25] COOL T A, SONG X M. Resonance ionization spectroscopy of HCO and DCO. II. The $\tilde{B}2A'$ state[J]. J Chem Phys, **96**(12): 8675-8683.